Hindawi
Journal of Sensors
Volume 2023, Article ID 9812126, 1 page
https://doi.org/10.1155/2023/9812126

Retraction

Retracted: A Systematic Pipelaying Control Method Based on the Sliding Matrix for Dynamically Positioned Surface Vessels

Journal of Sensors

Received 19 December 2023; Accepted 19 December 2023; Published 20 December 2023

This article has been retracted by Hindawi following an investigation undertaken by the publisher [1]. This investigation has uncovered evidence of one or more of the following indicators of systematic manipulation of the publication process:

(1) Discrepancies in scope
(2) Discrepancies in the description of the research reported
(3) Discrepancies between the availability of data and the research described
(4) Inappropriate citations
(5) Incoherent, meaningless and/or irrelevant content included in the article
(6) Manipulated or compromised peer review

The presence of these indicators undermines our confidence in the integrity of the article's content and we cannot, therefore, vouch for its reliability. Please note that this notice is intended solely to alert readers that the content of this article is unreliable. We have not investigated whether authors were aware of or involved in the systematic manipulation of the publication process.

Wiley and Hindawi regrets that the usual quality checks did not identify these issues before publication and have since put additional measures in place to safeguard research integrity.

We wish to credit our own Research Integrity and Research Publishing teams and anonymous and named external researchers and research integrity experts for contributing to this investigation.

The corresponding author, as the representative of all authors, has been given the opportunity to register their agreement or disagreement to this retraction. We have kept a record of any response received.

References

[1] X. Li, Z. Jin, and L. Wang, "A Systematic Pipelaying Control Method Based on the Sliding Matrix for Dynamically Positioned Surface Vessels," *Journal of Sensors*, vol. 2022, Article ID 9702532, 16 pages, 2022.

Hindawi
Journal of Sensors
Volume 2022, Article ID 9702532, 16 pages
https://doi.org/10.1155/2022/9702532

Research Article

A Systematic Pipelaying Control Method Based on the Sliding Matrix for Dynamically Positioned Surface Vessels

Xinfei Li,[1] Zhongyu Jin,[1] and Lihui Wang[2]

[1]*College of Shipbuilding Engineering, Harbin Engineering University, Harbin, Heilongjiang 150001, China*
[2]*College of Intelligent Systems Science and Engineering, Harbin Engineering University, Harbin, Heilongjiang 150001, China*

Correspondence should be addressed to Lihui Wang; wanglihui406@hrbeu.edu.cn

Received 21 October 2021; Revised 8 November 2021; Accepted 20 November 2021; Published 25 January 2022

Academic Editor: Wei Zhang

A pipelaying control method is presented in this paper which includes path planning, path guidance, and path tracking controller for dynamically positioned (DP) surface vessels based on the characteristics of the predefined path in marine pipelaying operation. The pipelaying control method depends on path coding, path selection logic system, and a sliding matrix. The sliding matrix contains a vessel local path and its specified control requirements, which can be updated by sliding down the waypoint table line by line as the vessel is traveling from one path to the next. A line of sight (LOS) algorithm is developed to calculate the desired vessel position and heading on a circular arc path. The motion controller, which can simultaneously control the vessel speed at the directions of surge and sway, is designed by decomposing the desired inertial resulting velocity into the desired body velocity components. A DP simulator for pipelaying operation is developed, and in order to verify the proposed method, a pipelaying simulation is carried out. The simulation results show that the proposed method enables the vessel to move along the desired path while maintaining a set crab angle, a specified speed, and a turning radius. The pipeline can be laid onto the specified waypoints even when the vessel is subjected to drift forces caused by ocean currents, wind, and waves.

1. Introduction

Over the last two decades, deep-water pipelaying has gone through a spectacular development and the present methods and trends in deep-water pipelay systems are described in [1] by Fossen. Three basic pipelay methods are commonly in use: S-lay, J-lay, and reeling which are described in [2, 3] by Heerema and Ai et al., respectively. Xu et al. [4] proposed a simple and feasible VFIFE model for the static and dynamic analysis of deepwater S-lay and J-lay pipelines. In order to realize the design of continuous pipe laying method of rolling pipe laying method, it is necessary to take into account the characteristics of pipe laying operation and the research of ship path tracking control method and organically combine the two to realize this method. The predecessors have not discussed the specific methods to realize continuous pipe laying, which will be described in this paper.

The path planning, path guidance, and path tracking of pipelaying vessels have their own unique characteristics. Firstly, it is difficult to follow the desired pipeline path precisely by indirectly controlling vessel position and heading [5, 6]. Secondly, it is necessary to consider the vessel position, heading, speed, and turning radius simultaneously during pipelaying operation because of pipelaying requirements. Guidance algorithm is an important part of ship path tracking control. It can provide the desired position, heading angle, speed, and other information for ship control and guide the ship to complete the relevant tracking tasks [7, 8]. Therefore, dynamic positioning (DP) control and pipeline dynamics are the two main parts of the deepwater pipelaying simulation model [3].

The desired pipe paths consist of a few straight-line paths. In order to achieve a smooth transition between two straight-line paths, a circular arc path is inserted between the adjacent straight-line paths. The methods used to generate such circular arc path have been extensively studied in recent years, and the Dubins path is highly recognized in [9]. The curvature of the Dubins path is usually discontinuous at the intersection of a straight-line path and its adjacent

circular arc path. Accordingly, the Pythagorean hodographs [10] and the clothoid arcs [11] had been developed to obtain path with continuous curvature. Lekkas and Fossen [12] proposed the monotonic cubic Hermit spline interpolation (MCHSI) to realize the continuous change of path curvature with low computational cost in ship path planning. However, it is not easy to lay the pipe onto the desired pipeline path by indirectly controlling vessel path. Fu et al. [5, 13] developed a method of path analysis and mapping relation between the desired pipeline path and the desired vessel path and used sliding mode control to study the tracking control of pipe laying operation of pipelaying ship [14]. Rout et al. [15] presents a modified line-of-sight (LOS) guidance law and an adaptive neural network (NN) controller for underactuated marine vehicles in the presence of uncertainties and constraints. Lekkas and Fossen [16, 17] proposed a time-varying lookahead-distance LOS method. When the vessel moves close to the desired path, the heading is gradually adjusted to the desired direction, which is beneficial for reducing the overshoot and oscillation of the vessel position. Among all existing methods, the sideslip motion is easy to occur during path-following due to environmental interferences. Therefore, a nonlinear adaptive path-following controller is proposed by Fossen et al. [18] to compensate for vessel sideslip. For the plane path tracking problem of underactuated ships, Peymani and Fossen [19] designed a dynamic controller by using the idea of integral backstepping, explicitly considering the geometric error and ensuring the path convergence. In addition, aiming at the linear path tracking problem of fully driven ships, they derived the control law using the least square method and adjusted the ship speed according to the geometric distance and the convergence speed of the path [20]. Moe et al. [21] developed a guidance and control system for underactuated surface vessels to solve the control objective of making the vessel to follow a curved path in the presence of unknown ocean currents. Heshmati-Alamdari et al. [22] presented a robust nonlinear model predictive control (NMPC) scheme for the case of underactuated autonomous underwater vehicles (AUVs). Nie and Lin [23] proposed an adaptive fuzzy path following control law, which is based on the improved adaptive integrated line of sight (IAILOS) guidance law for the control of underactuated ship in the case of time-varying ocean current and sideslip. Abdurahman et al. [24] used path-following control and speed allocation to solve the three-dimensional path-following problem of underactuated underwater vehicles. Path-following control was achieved by defining a slip angle relative to the desired heading angle. Lamraoui and Zhu [25] presented an improved active disturbance rejecter control (ADRC) for path-following control of autonomous underwater vehicles under significant fast-varying disturbances caused by waves and sea currents. Du et al. [26] established a robust nonlinear control law by using disturbance observer, auxiliary power system, and dynamic surface control (DSC) technology to keep the ship's position and heading at the expected value. Yu et al. [27] presented an improved guidance law that transforms 3D path-following errors into controlled speed errors and designed a simplified nonlinear single-input fuzzy controller against unknown disturbances. Huang et al. [28] presented a 2D path-following control method for autonomous underwater vehicles (AUVs) based on dynamic circle heading modification (DCHM). Loginov et al. [29] proposed special control functionality for trailing suction dredgers in dynamic positioning (DP) systems that focused mainly on the dredging track controller, and the method was verified by the simulation and sea-trial results. Shi et al. [5, 30] presented a pipelaying control method for DP vessels, and it was tested in the pipelaying operation. Here, it refers to the control method. Healey and Lienard [31] designed the autopilot of the six degree of freedom underwater vehicle through sliding mode control, which has a good response to the speed, steering, and heave motion of the low-speed AUV. Mu et al. [32] investigated the path-following control problem for an underactuated unmanned surface vehicle (USV) in the presence of dynamical uncertainties and time-varying external disturbances. Rout and Subudhi [33] designed an explicit model predictive controller (Ex-MPC) for implementing a LOS guidance law.

The pipeline dynamic model is the other key and important problem in pipelaying operation. Ai et al. [3] proposed a pipelaying nonlinear dynamic model, which integrates the major aspects related to numerical simulation, including coupled pipeline motion and roller contact forces. Jensen [34, 35] proposed a nonlinear dynamic model which was capable of undergoing shearing, twist, and bending for the pipe string, and the model is suitable for pipelaying operations by a dynamically positioned surface vessel. Szczotka [36] studied a dynamic and quasi-static model that showed the high dynamic forces in the pipelaying equipment during pipelaying simulation operated in the sea for analysis of a pipelay spread. Different pipelaying models were studied in the above. However, applications of this method to pipelaying operation, especially for a series of waypoints, are not discussed in detail. In order to study a pipelaying system with DP vessels in time domain, it is necessary to simplify appropriately the pipeline dynamic model.

In this study, a systematic method, including path planning, guidance algorithm, and path tracking for pipelaying vessels, is presented from the prospect of the whole DP control system. One of the key steps to achieve path tracking finally is to combine the desired path information and the guidance algorithm with control strategy. The realization of the system depends on the coding method of the pipeline desired path. The method of sliding matrix is proposed to extract the required path information from the waypoint table for continuous pipelaying at specified speed, heading, and turning radius. The sliding matrix contains the vessel local desired path, the desired crab angle, and turning radius and the desired pipelaying speed. A simple and reliable guidance algorithm is also designed for circular arc paths of the pipelaying vessel, which is convenient for the guiding system to execute quickly. Then, the vessel speed and the yaw controllers are also designed. Finally, the effectiveness of the proposed control method of pipelaying control is verified using a DP simulator.

2. The Method of Pipelaying Path Based on a Sliding Matrix

2.1. Definition of Coordinates. Two coordinate systems adopted to define ship motions are presented in this section first. The North-East-Down (NED) coordinate system $\{n\} = (x_n, y_n, z_n)$ with origin o_n defined relative to the Earth's reference ellipsoid. It is usually defined as the tangent plane on the surface of the Earth moving with the marine craft. x_n axis points towards true north, y_n axis points towards east, and z_n axis points downwards from the Earth surface to its geocentric. This is usually referred to as flat Earth navigation, and it can be simply denoted by $\{n\}$, as shown in Figure 1.

The body-fixed reference frame $\{b\} = (x_b, y_b, z_b)$ with origin o_b is a moving coordinate frame that is fixed to the craft, and it can be simply denoted by $\{b\}$. The body axes are chosen to coincide with the principal axes of inertia, as shown in Figure 2. The x_b is the longitudinal axis pointing from aft to fore. The y_b is the transversal axis pointing to starboard. The z_b is the normal axis pointing from top to bottom.

2.2. Waypoints and Its Coding Method for Pipelaying Paths. The desired path of pipeline to be laid is expressed as a set of waypoints. The waypoint table for pipelaying contains the information of all waypoints, including north and east coordinates, crab angle, laying speed, and turning radius of pipeline, as shown in Table 1.

The waypoint table gives a detailed expression of the characteristics of each segment of pipelaying paths, and it also specifies the control requirements of the pipelaying vessel. The pipelaying paths are divided into several straight-line segments which are separated by different waypoints. As shown in Table 1, N_k and E_k are the north coordinate and east coordinate of the waypoint P_k, respectively. γ_k represents the crab angle which is a fixed angle between the desired vessel heading and the path tangential direction. V_k represents the desired pipelaying speed when the vessel is tracking the desired straight-line pipe path P_kP_{k+1} which is also represented by S_k. R_k represents the turning radius of the desired pipe circular arc path C_k, so as to obtain a smooth circular arc transition between a straight-line path to its adjacent next straight-line path, as shown in Figure 3.

In order to make the analysis of pipelaying path easier and achieve automatic identification in path tracking by programming, all the straight-line and circular arc paths in Figure 3 need to be coded.

As shown in Figure 3, P_k, $k = 1, \cdots, n$ denotes the waypoint k. A straight-line path is denoted as S_k, $k = 1, \cdots, n-1$, and S_1 represents the first straight-line path P_1P_2. A circular arc path is denoted as C_l, $l = 1, \cdots, n-2$, and C_1 represents the first circular arc path between S_1 and S_2. χ_1 is the path-tangential angle between the desired pipe straight-line path P_1P_2 (S_1) and x_n axis of $\{n\}$. γ_1 is the set crab angle, which is a specified angle between the desired vessel heading and the tangential direction of the straight-line path.

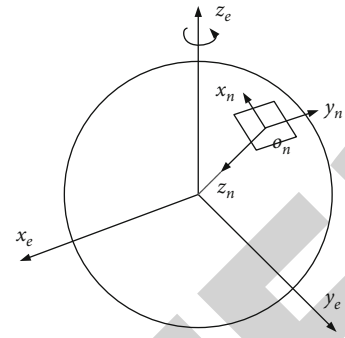

Figure 1: NED reference frame.

2.3. Pipelaying Path Planning Based on the Sliding Matrix. The desired paths of pipeline usually consist of straight-line paths and circular arc paths in sequence. For a straight-line path, it is only necessary to consider the start point and end point whereas for a circular arc path, the circular arc center also needs to be considered. A sliding matrix may be constructed using the information in the waypoint table.

As shown in Figure 3, the desired vessel heading ψ_k for straight-line path S_k is obtained by

$$\psi_k = \chi_k + \gamma_k, \tag{1}$$

where χ_k is the path-tangential angle of the desired pipe path S_k relative to χ_n axis of $\{n\}$. γ_k is the set crab angle when the vessel is tracking S_k.

As shown in Table 1, the control information of a sliding matrix is composed of a set of waypoints. The sliding matrix slides down the waypoint table and traverses all waypoints during pipelaying operation, as shown in Table 2.

The sliding matrix used to calculate the guidance law is proposed to resolve path-tracking problem in pipelaying operation. The sliding matrix, three rows and five columns, includes position coordinates of three waypoints, the desired heading angle, the desired speed of straight-line path, and the desired turning radius of circular arc path. From Table 2, the second column contains north coordinates of three waypoints, the third column contains east coordinates of three waypoints, the fourth column contains the desired heading, the fifth column contains the desired pipelaying speed of straight-line path, and the sixth column contains the desired turning radius.

The turning radius of pipelaying is related to characteristics of the pipeline, the gyration radius of the pipelaying vessel, and desired pipelaying speed on circular arc paths. The circular arc path represents the natural circular arc path when the vessel is traveling from one straight-line path to the next one at a specified turning radius and speed. The desired state of the start point of the circular arc path is $q_1 = (N_{q_1}, E_{q_1}, \psi_{q_1})$, and the desired state of the end point is $q_2 = (N_{q_2}, E_{q_2}, \psi_{q_2})$.

The steps for the analysis of the path based on sliding matrix are as follows:

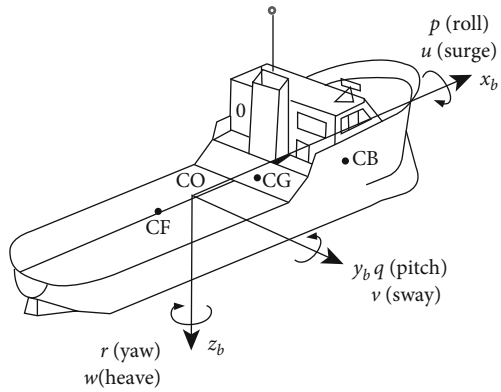

Figure 2: Body-fixed reference frame.

Table 1: The waypoint table for pipelaying operation.

No.	North	East	Crab angle	Speed	Turn radius
1	N_1	E_1	—	—	—
2	N_2	E_2	γ_1	V_1	—
3	N_3	E_3	γ_2	V_2	R_1
...	...	...	...	...	...
k	N_k	E_k	γ_{k-1}	V_{k-1}	R_{k-2}

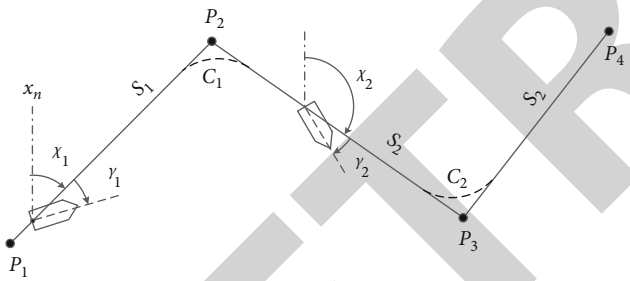

Figure 3: The coding method of the pipelaying path.

Table 2: The control information of a sliding matrix.

No.	North	East	Heading	Speed	Turn radius
k	N_k	E_k	—	—	—
$k+1$	N_{k+1}	E_{k+1}	ψ_k	V_k	—
$k+2$	N_{k+2}	E_{k+2}	ψ_{k+1}	V_{k+1}	R_k

Step 1. To calculate the angle between two adjacent straight-line paths.

The sketch of desired pipelaying paths is shown in Figure 4. Here, χ_2 is the path-tangential angle between P_2 P_3 (S_2) and the x_n axis of $\{n\}$. α_1 is the angle between the two straight-line paths S_1 and S_2.

The calculation method of α_1 is related to the rotation direction of circular arc path. When $0 \le \chi_1 < \pi$, the angle between P_1P_2 and P_2P_3 can be obtained using

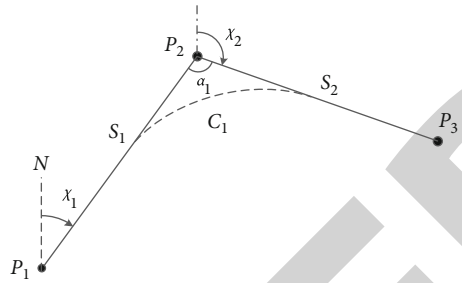

Figure 4: Sketch diagram of the angle between pipe paths.

$$\alpha_1 = \begin{cases} \pi - (\chi_1 - \chi_2)\mathrm{rg} = 0 & 0 \le \chi_2 < \chi_1, \\ \pi - (\chi_2 - \chi_1)\mathrm{rg} = 1 & \chi_1 \le \chi_2 < \chi_1 + \pi, \\ \chi_2 - (\chi_1 + \pi)\mathrm{rg} = 0 & \chi_1 + \pi \le \chi_2 < 2\pi, \end{cases} \tag{2}$$

where $\mathrm{rg} = 1$ implies that the rotation direction of a circular arc path is clockwise and $\mathrm{rg} = 0$ implies that the rotation direction is counterclockwise.

When $\pi \le \chi_1 < 2\pi$, the value of angle α_1 between the two straight-line paths can be obtained using

$$\alpha_1 = \begin{cases} (\chi_1 - \pi) - \chi_2\mathrm{rg} = 1 & 0 \le \chi_2 < \chi_1 - \pi, \\ \chi_1 - \chi_2\mathrm{rg} = 0 & \chi_1 - \pi < \chi_2 < \chi_1, \\ \pi - (\chi_2 - \chi_1)\mathrm{rg} = 1 & \chi_1 < \chi_2 \le 2\pi. \end{cases} \tag{3}$$

Step 2. To calculate the distance between a waypoint point and its tangent point.

To calculate the distance between a waypoint point and its adjacent tangent point, the sketch is shown in Figure 5. As shown in Figure 5, O_1 is the center of the circular arc path C_1, and R_1 is the turning radius. The points, q_1 and q_2, are the tangent points between the circular arc path and its two adjacent straight-line paths, respectively. θ_{Oq_1} is the angle between the vector O_1q_1 and x_n axis of $\{n\}$. θ_{Oq_2} is the angle between the vector O_1q_2 and x_n axis of $\{n\}$.

It is straightforward to calculate the distance between the waypoint P_2 and the tangent point q_1, which can be expressed as L_{2q_1}. Similarly, L_{1q_1} is the distance between the waypoint P_1 and q_1. Additionally, L_{2q_1} is equal to L_{2q_2}. It is assumed that R_1 and α_1 are known and consequently, L_{2q_1} can be expressed as

$$L_{2q_1} = L_{2q_2} = \frac{R_1}{\tan(\alpha_1/2)}. \tag{4}$$

Step 3. To calculate the coordinates of the tangent points.

Let L_{12} denote the distance between the waypoint P_1 and P_2. Hence, L_{1q_1} can be obtained from

$$L_{1q_1} = L_{12} - L_{2q_1}. \tag{5}$$

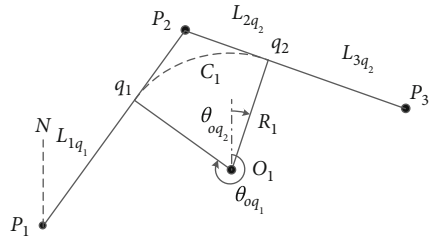

Figure 5: Sketch of the desired pipelaying path.

Here, it is necessary to make sure that $L_{12} > L_{2q_1}$ when the waypoints are specified.

Thereafter, the coordinates of the center of C_1, O_1 satisfy

$$\begin{bmatrix} N_{O_1} \\ E_{O_1} \end{bmatrix} = \begin{bmatrix} \cos\chi_{S_1} & -\sin\chi_{S_1} \\ \sin\chi_{S_1} & \cos\chi_{S_1} \end{bmatrix} \begin{bmatrix} L_{1q_1} \\ L_{Oq_1} \end{bmatrix} + \begin{bmatrix} N_1 \\ E_1 \end{bmatrix}. \quad (6)$$

Here, L_{Oq_1} is the vertical distance between the tangent point q_1 and the center O_1. For a clockwise circular arc path, L_{Oq_1} equals to R_1, and for a counterclockwise circular arc path, L_{Oq_1} equals to $-R_1$.

The coordinates of the tangent point q_1 satisfy

$$\begin{bmatrix} N_{q_1} \\ E_{q_1} \end{bmatrix} = \begin{bmatrix} \cos\chi_{S_1} & -\sin\chi_{S_1} \\ \sin\chi_{S_1} & \cos\chi_{S_1} \end{bmatrix} \begin{bmatrix} L_{1q_1} \\ 0 \end{bmatrix} + \begin{bmatrix} N_1 \\ E_1 \end{bmatrix}. \quad (7)$$

Consequently, the coordinates of the tangent point q_2 satisfy

$$\begin{bmatrix} N_{q_2} \\ E_{q_2} \end{bmatrix} = \begin{bmatrix} \cos\chi_{S_2} & -\sin\chi_{S_2} \\ \sin\chi_{S_2} & \cos\chi_{S_2} \end{bmatrix} \begin{bmatrix} L_{2q_2} \\ 0 \end{bmatrix} + \begin{bmatrix} N_2 \\ E_2 \end{bmatrix}. \quad (8)$$

Step 4. To calculate the angle between two straight lines.

The angle range is chosen to represent the part of a circular arc pipe path, as shown in Figure 5. Accordingly, it is necessary to calculate the angle between two straight lines connecting two tangent points to the center of the circular arc path. Moreover, it is also used to calculate the LOS point if it is required. In order to ensure angle continuity as a circular arc path passes across x_n axis of $\{n\}$, it is necessary to analyze the angle ranges of θ_{Oq_1} and θ_{Oq_2} further.

When $\theta_{oq_2} > \theta_{oq_1}$, it implies that the angle range of the circular arc path does not contain zero point, and the circular arc path does not pass across x_n axis of $\{n\}$. Whereas when $\theta_{oq_2} < \theta_{oq_1}$, it implies that the angle range of the circular arc path contains zero point, and the circular arc path passes across x_n axis of $\{n\}$.

Hence, the relationship mentioned above can be expressed as

$$\begin{cases} \theta'_{oq_1} = \theta_{oq_1} \\ \theta'_{oq_2} = \theta_{oq_2} \end{cases} \text{rg} = 1, \theta_{oq_2} > \theta_{oq_1} \text{ or } \text{rg} = 0, \theta_{oq_2} < \theta_{oq_1}. \quad (9)$$

Here, θ'_{oq_1} and θ'_{oq_2} are the updated values of θ_{oq_1} and θ_{oq_2}, respectively.

Consequently, Equations (10) and (11) are obtained:

$$\begin{cases} \theta'_{oq_1} = \theta_{oq_1} - 2\pi \\ \theta'_{oq_2} = \theta_{oq_2} \end{cases} \text{rg} = 1, \theta_{oq_2} < \theta_{oq_1}, \quad (10)$$

$$\begin{cases} \theta'_{oq_1} = \theta_{oq_1} \\ \theta'_{oq_2} = \theta_{oq_2} - 2\pi \end{cases} \text{rg} = 0, \theta_{oq_2} > \theta_{oq_1}. \quad (11)$$

2.4. Mapping from the Desired Pipelaying Path to the Desired Vessel Path. The horizontal projection distance between the pipe touchdown point at seabed and the vessel rotation center during pipelaying operation is defined as the touchdown distance. The desired vessel path needs to be calculated so that the pipe touchdown point can be placed on the desired path during turning in pipelaying operation. It is necessary to estimate the desired vessel path from the pipeline desired path and the touchdown distance. The touchdown distance can be modified anytime if it is necessary during pipelaying operation. The touchdown distance is mainly influenced by the method of pipelaying operation, sea depth, pipe mechanical properties, etc. The desired vessel path can be calculated based on the desired pipelaying path, and their geometric relationship is shown in Figure 6.

V_1 is the desired pipelaying speed when tracking S_1. ψ_{C_1}, V_{C_1}, and β_{C_1} are the desired heading angle, pipelaying speed, and sideslip angle when tracking the path C_1, respectively. R_V and R_1 are the radius of the desired circular path of the DP vessel and pipeline, respectively. L_{td} is the touchdown distance. P_{s_1} and P_{s_2} are the start point and end point of the path C_1, respectively. P_L is the LOS point on the path C_1. θ_{OL} is the azimuth angle of the straight-line O_1P_L.

The desired pipeline paths are composed of a few straight-line paths and circular arc paths in sequence. It is necessary to control precisely the ship heading angle to make smooth progress of pipelaying operation when the pipelaying vessel runs along the desired path. When the value of the crab angle is set to 0, the desired vessel heading angle is equal to the tangent direction of pipeline path; when the crab angle is a constant value, the desired vessel heading angle is obtained using Equation (1).

2.4.1. To Calculate the Desired Vessel Path from a Desired Straight-Line Pipe Path. Let $q_1(x_1, y_1)$ and $q_2(x_2, y_2)$ denote the start point and end point of the circular arc path of pipeline, respectively, χ_1 denotes the straight path angle, and L_{td} denotes the touchdown distance. Let $P_{s_1}(x_{s_1}, y_{s_1})$ and $P_{s_2}(x_{s_2}, y_{s_2})$ denote the start point and end point of the circular arc path of vessel, respectively. Accordingly, the coordinates of $P_{s_1}(x_{s_1}, y_{s_1})$ can be obtained using Equation (12), as shown

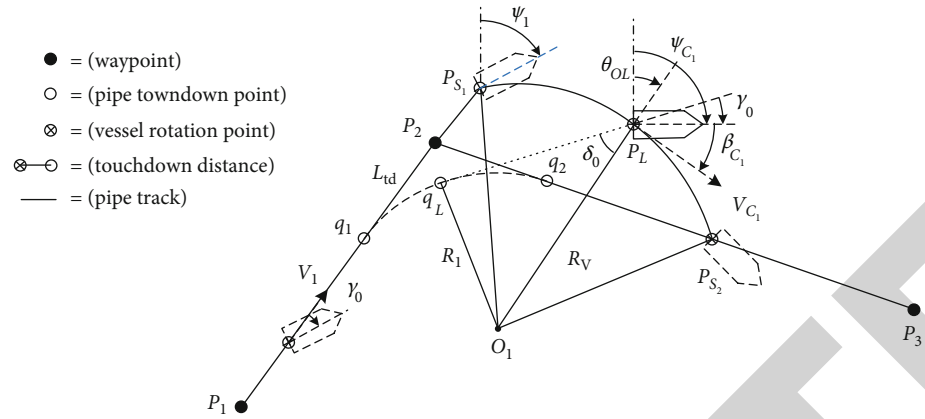

Figure 6: Mapping relationship between the desired vessel path and pipelaying path.

in Figure 6.

$$\begin{cases} x_{s_1} = x_1 + L_{\text{td}} \cos \chi_1, \\ y_{s_1} = y_1 + L_{\text{td}} \sin \chi_1. \end{cases} \tag{12}$$

Consequently, the coordinates of $P_{s_2}(x_{s_2}, y_{s_2})$ can be obtained using

$$\begin{cases} x_{s_2} = x_2 + L_{\text{td}} \cos \chi_2, \\ y_{s_2} = y_2 + L_{\text{td}} \sin \chi_2. \end{cases} \tag{13}$$

In this study, when the crab angle is set to 0, the desired vessel heading angle is equal to the tangent angle of desired pipeline paths.

2.4.2. To Calculate the Desired Vessel Path from a Desired Circular Arc Pipelaying Path. The desired circular arc path of pipe to be laid should be tangent to its adjacent straight-line path. This means that the desired vessel circular path is not tangent to its adjacent vessel straight-line path. Here, all crab angles for the desired straight-line and circular arc paths are set to γ_0. Accordingly, the desired heading angle for the first desired straight-line pipeline path is obtained using Equation (14), as shown in Figure 6.

$$\psi_1 = \chi_1 + \gamma_0, \tag{14}$$

where ψ_1 is the desired heading when tracking the straight-line path S_1 and γ_0 is the set crab angle.

When the vessel is tracking the circular arc path C_1, the desired heading angle ψ_{C_1} can be expressed as

$$\psi_{C_1} = \begin{cases} \theta_{OL} + \delta_0 + \gamma_0 & \text{Clockwise path}, \\ \theta_{OL} - \delta_0 + \gamma_0 & \text{Counterclockwise path}. \end{cases} \tag{15}$$

Here, the crab angle γ_0 is a constant during pipelaying operation.

The value of δ_0 can be obtained using

$$\delta_0 = \arcsin \frac{R_1}{R_{\text{V}}}. \tag{16}$$

Hence, the relationship between the desired turning radius of DP vessel and the desired turning radius of pipeline path can be expressed as

$$R_{\text{V}} = \sqrt{R_1^2 + L_{\text{td}}^2}. \tag{17}$$

Here, L_{td} is the touchdown distance.

2.5. A Guidance Law of Circular Arc Paths for DP Vessels. It is necessary to construct a guidance system that is suitable for DP vessels so that the vessel actual path can converge to the desired path smoothly. The common LOS guidance law is only suitable for path following of straight-line or circular arc path for underactuated water surface ships or underwater vehicles. Therefore, a new LOS guidance algorithm of circular arc paths for DP vessels is presented.

2.5.1. The Guidance Law for a Straight-Line Path. Let $P_{\text{L}}(N_{\text{LOS}}, E_{\text{LOS}})$ be the desired LOS point on a straight-line path. The points (N_k, E_k) and (N_{k+1}, E_{k+1}) are the start point and end point of the straight-line path, respectively. Let (N_t, E_t) be the real-time position of DP vessels. Thereafter, the following relationship can be obtained.

$$\begin{aligned} (N_{\text{LOS}} - N_t)^2 + (E_{\text{LOS}} - E_t)^2 &= R_{\text{LOS}}^2, \\ \tan \alpha_k = \frac{\Delta E}{\Delta N} = \frac{E_{k+1} - E_k}{N_{k+1} - N_k} &= \frac{E_{\text{LOS}} - E_k}{N_{\text{LOS}} - N_k}, \end{aligned} \tag{18}$$

where R_{LOS} is the radius of the LOS guidance law specified by the practice requirements.

2.5.2. A Guidance Algorithm for Circular Arc Paths. The guidance law of a curved path also takes the vessel position as the center and makes a circle with a radius value based on the principle of LOS guidance law of the straight-line path. One of the intersections of the circle and the circular

arc path is chosen as the LOS point. Meanwhile, the direction of the desired resultant speed of the vessel passes through the LOS point. The schematic diagram of the LOS guidance algorithm of the circular arc path is shown in Figure 7.

As shown in Figure 7, P_L denotes the LOS point on the desired vessel circular arc path. p_s denotes the real-time position of the vessel set rotation center. O_1 denotes the center of C_1. θ_{OL} denotes the azimuth angle of O_1P_L, and b denotes the angle between O_1P_C and x_n axis of $\{n\}$. σ_C is the angle between O_1P_C and O_1P_L.

It is necessary to know the angle of the straight-line segment connecting the LOS point and the circle center O_1P_L for calculating the coordinates of the LOS point on the circular arc path.

The following relationship between θ_{OL} and b can be obtained from Figure 7.

$$\theta_{OL} = \sigma_C - b. \tag{19}$$

The value of the angle σ_C is calculated using

$$\sigma_C = \frac{\pi}{2} - \delta_0. \tag{20}$$

The value of the angle b can be obtained using

$$b = \begin{cases} \theta_{OC} & 0 < \theta_{OC} < \dfrac{\pi}{2}, \\ \theta_{OC} - \dfrac{\pi}{2} & \dfrac{\pi}{2} < \theta_{OC} < \pi, \\ \theta_{OC} - \pi & \pi < \theta_{OC} < \dfrac{3\pi}{2}, \\ 2\pi - \theta_{OC} & \dfrac{3}{2}\pi < \theta_{OC} < 2\pi. \end{cases} \tag{21}$$

Thereafter, the coordinates of LOS point on a circular arc path can be obtained using

$$\begin{cases} N_{LOS} = N_{O_1} + R_L \cos(\theta_{OL}), \\ E_{LOS} = E_{O_1} + R_L \sin(\theta_{OL}). \end{cases} \tag{22}$$

The LOS point is the desired vessel position on a desired path. Hence, the desired heading angle during the circular path following can be obtained using Equation (15).

3. Control System Designing for Pipelaying Operation

As shown in Figure 8, the pipelaying simulation system of DP vessels is constructed, which includes the waypoint table, path planning module, path guidance module, thrust allocation module, propeller system module, vessel hydrodynamic module, environment force module, state observer module, and motion controller.

The data transmitted between the modules are represented by the numbers and ①—the coordinates, heading angle, laying speeds, turning radius; ②—the desired vessel path; ③—the desired LOS point, speed, heading; ④—the desired forces; ⑤—the desired thrusts; ⑥—the actual sum forces; ⑦—the estimated wind loads; ⑧—the LOS point.

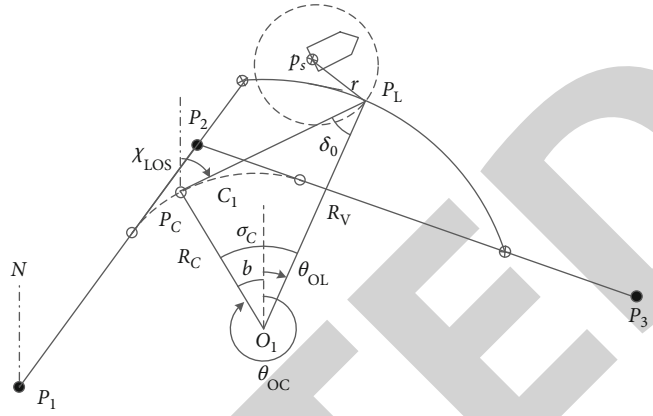

Figure 7: A LOS guidance algorithm for a circular arc path.

The principle of pipelaying operation of the DP simulation is presented as follows:

(1) The waypoint coordinates, crab angle, pipelaying speed, and turning radius of the pipe are input in the waypoint table according to the operational requirements of a pipelaying task

(2) The desired pipelaying path, the desired vessel path, and heading angle are generated by the path planning module from the waypoint table. Then, they are input into the path guidance module

(3) The vessel real-time position, speed, and heading angle are input into the module of state filter and observer, and the vessel drift (Low Frequency, LF) motion is estimated by filtering out the first-order wave-induced (Wave Frequency, WF) motion

(4) The LOS point is calculated using the path guidance module by inputting the vessel real-time position, heading angle and speed, the desired vessel path, and control requirements. Then, the LOS points are input into the motion controller module

(5) The desired forces in three degrees of freedom are estimated by the motion controller module through calculating the deviation between LOS point and estimated real-time motion. Then, they are input into the thrust allocation module

(6) The desired thrust and the azimuth angle of each thruster are calculated according to the configuration of the propulsion system and thrust allocation method chosen by the DP operator

(7) The actual thrust vector is generated by each thruster according to the desired thrust and azimuth angle

(8) The propeller system produces the sum forces in three degrees of freedom through the actual thrust vectors. Then, the sum forces will be applied to the DP vessel

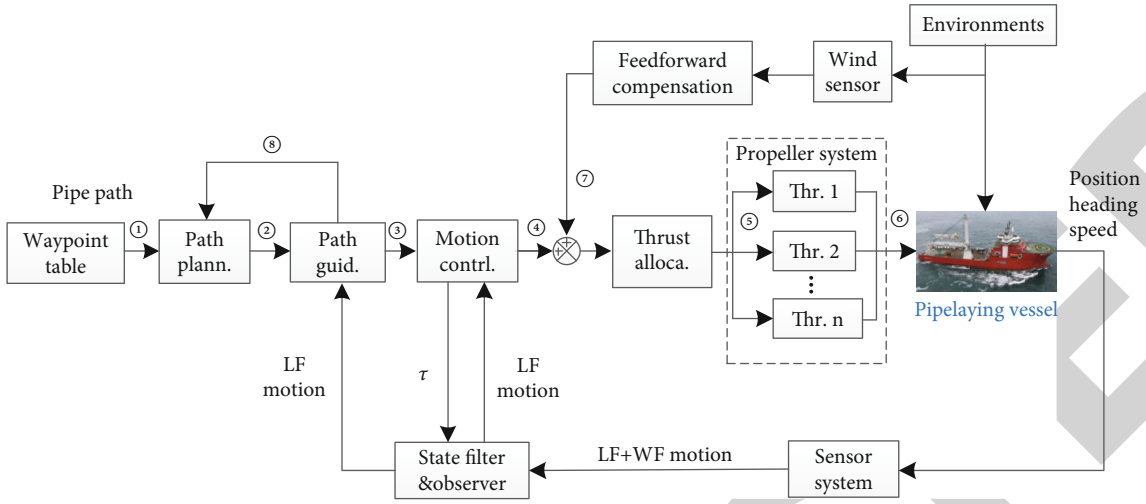

Figure 8: DP simulation system for a pipelaying vessel.

(9) The DP vessel is moved along the desired path at the given speed and heading angle by the pipelaying controller, even the vessel is exposed to the drift forces caused by ocean currents, wind, and waves

3.1. Path Selection Method in the Pipelaying Operation. The desired path of the pipelaying vessel can be obtained by making use of the waypoint table and mapping relationship between the pipelaying path and the vessel path. Hence, it is necessary to know the type of pipe path it is traveling along so the corresponding LOS point of the pipelaying vessel can be calculated. The flow chart of the path selection method is shown in Figure 9, and the details are explained in the following:

(1) Specify an index number for each straight-line path and each circular arc path of the pipelaying vessel, as well as the initial LOS point. And the first point in the waypoint table is usually set as the initial LOS point

(2) Let k and l be the indices for a straight-line path and a circular arc path, respectively. And the initial values are set as $k = 1$, $l = 0$

(3) The sliding matrix is generated according to the waypoint table and the initial value of k

(4) The desired pipelaying path expressed by the sliding matrix is analyzed to determine the end point of straight-line path and circular arc pipe path, the circle center, and rotation direction of the circular arc path of pipeline. The desired vessel path is calculated from the desired pipelaying path

(5) Determine which path type the vessel is going to track when the present path range is exceeded by the pipelaying vessel

(6) The condition $k > l$ implies that the vessel is going to travel along a straight-line path, and when $k = l$, it implies that the vessel is going to travel along a circular arc path

(7) When the vessel is traveling along a straight-line path and does not exceed its range, the start and the end points of the straight-line path are output to the LOS point calculating module. When the straight-line path range is exceeded, i.e., the vessel has just reached a circular arc path, then set $l = l + 1$. Consequently, now $k = l$, and the LOS point on the circular arc path is calculated

(8) When the vessel is traveling along a circular arc path and exceeds its range, it implies that the vessel has just reached the next straight-line path, then set $k = k + 1$. Consequently, now $k > l$, it is necessary to update the sliding matrix, and it will continue to run from the third step

It can be summarized as follows: when the value of k is increased by one, the sliding matrix is required to be updated and path analysis is also performed so that the related parameters of the next path are obtained. When the value of l is increased by one, the sliding matrix is not required to be updated. However, it is necessary to determine whether the vessel is sailing on a straight-line path or a circular arc path, and the related LOS point is required to be calculated.

3.2. Coordinate Calculation of LOS Point. The LOS point is defined as the desired vessel position on a specified path. It is a dynamically changing point that guides the vessel approach to the desired path along with a specified heading. The vessel path selection is based on the previous LOS point. The flow chart for calculation of LOS points is shown in Figure 10 and is explained in the following:

(1) The initializing parameters are input into LOS point calculating module

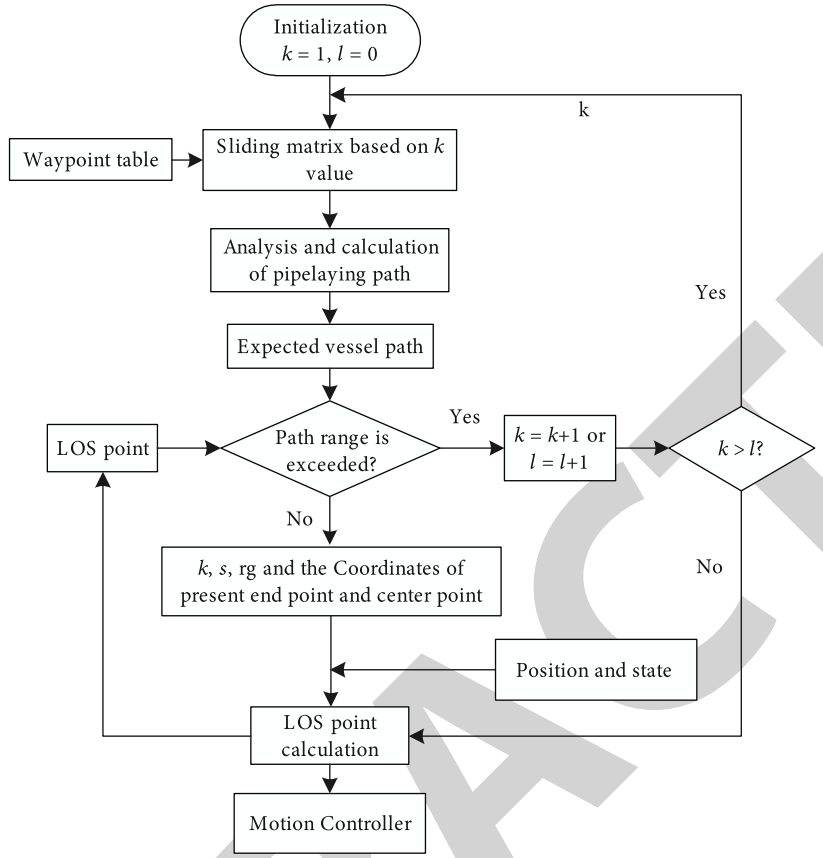

Figure 9: Execution process of the path selecting method.

(2) Check whether the path is required to be updated by comparing the value of k and k_{pre} in the process of calculating LOS point

(3) The condition $k = k_{pre}$ implies that the path does not need to be updated, where k is the index value of the present straight-line path and k_{pre} is the index value of the previous straight-line path

(4) When $k > k_{pre}$, it implies that the path is required to be updated, and the start and the end points of a straight-line path are also required to be recalculated and updated

(5) Determine the type of vessel path by comparing the values of k and l. If $k > l$, it implies that it is a straight-line path, and the method used to calculate LOS point of a straight-line path should be chosen. If $k = l$, it implies that it is a circular arc path, and the method used to calculate LOS point of a circular arc path should be selected

(6) The LOS point of the desired vessel path is obtained

3.3. Multiobjective Motion Controller of DP Vessels. The LOS point is the desired position of the ship moving on the desired path during path following, and its coordinates are changing dynamically when the vessel reaches a new position. The sliding matrix also contains such control requirement information which is obtained by the waypoint table. The diagram of the multiobjective controller of a DP vessel is shown in Figure 11.

When the vessel real-time position and the LOS point are known, the deviation of the vessel position in $\{n\}$ coordinate frame is converted into the deviation in $\{b\}$ coordinate frame. Then, the desired surge force, sway force, and yaw moment of the vessel can be calculated in combination with the deviations of the vessel speed and heading. The deviations of position and heading angle in $\{b\}$ can be obtained using

$$\begin{cases} \tilde{N} = N_{los} - N, \\ \tilde{E} = E_{los} - E, \\ \tilde{\psi} = \psi_d - \psi, \end{cases} \tag{23}$$

where $\tilde{N}$ and $\tilde{E}$ are the deviations of north and east positions, respectively. $\tilde{\psi}$ is the deviation of the heading angle. N and E are the real-time north and east positions, respectively; ψ is the real-time heading angle.

Hence, when the vessel is tracking the first desired circular arc path, the desired body velocity components decomposed from the pipelaying speed in the coordinate frame $\{n\}$ can be expressed as

$$\begin{cases} u_d = \cos\left(\beta_{C_1}\right) V_d, \\ v_d = \sin\left(\beta_{C_1}\right) V_d, \end{cases} \tag{24}$$

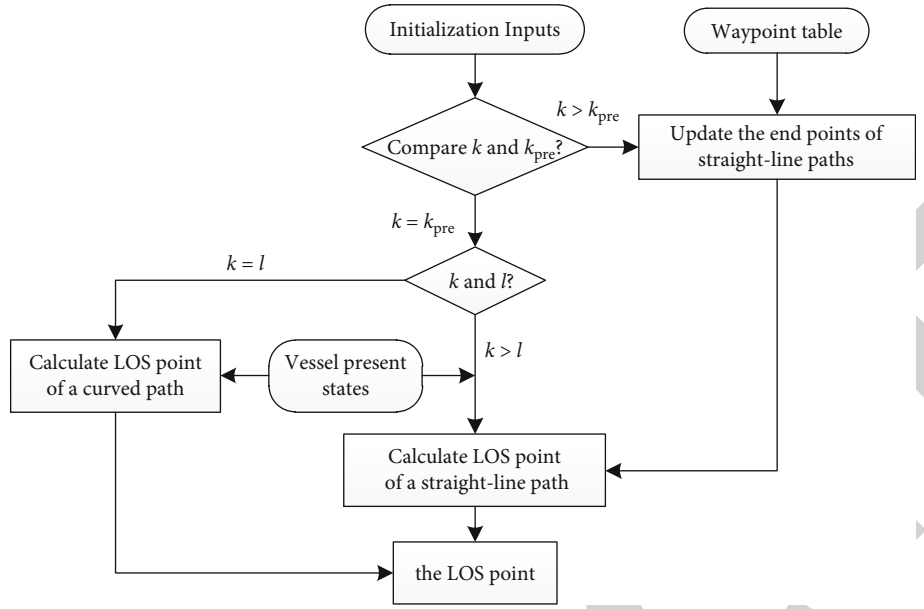

Figure 10: The calculation process of the LOS point.

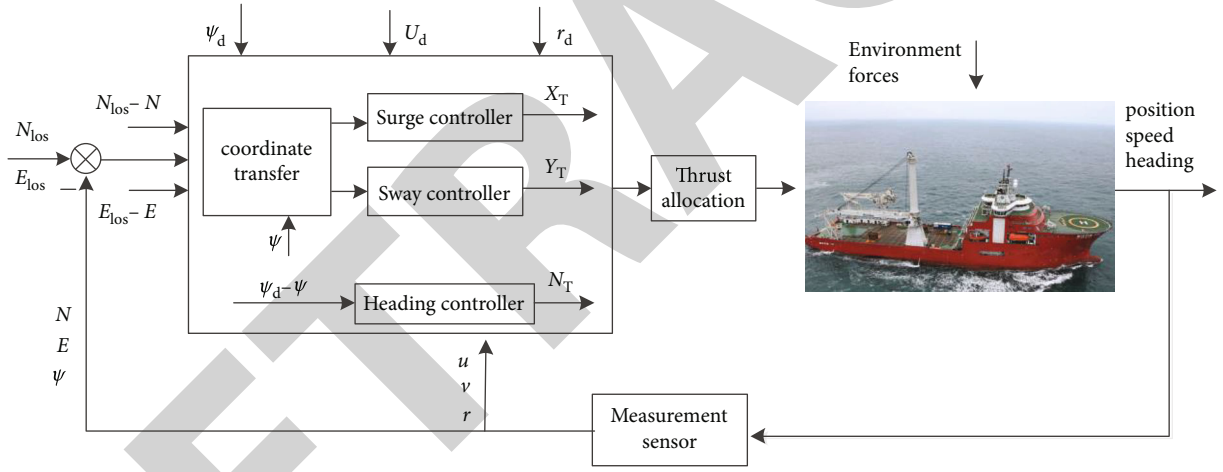

Figure 11: Multiobjective controller of DP vessel.

Table 3: The waypoint table of the pipelaying operation.

No.	N (m)	E (m)	Crab angle (degree)	Speed (m/s)	Turn radius (m)
1	0	0	0	2	0
2	1000	1000	0	2	300
3	1000	2000	0	2	300
4	200	2600	0	2	300
5	500	4000	0	2	300
6	1500	4100	0	2	0

where V_d is the desired speed in the coordinate frame $\{n\}$; β_{C_1} is the desired sideslip angle; u_d and v_d are the desired velocity components in the body coordinate frame, respectively.

When the vessel is tracking the desired circular arc path, the desired vessel speed is obtained using

$$V_d = V_{C_1}. \tag{25}$$

From Figure 6, when the rotational direction is clockwise and the circular arc path is clockwise, the value of β_{C_1} is obtained by

$$\beta_{C_1} = \frac{\pi}{2} - \delta_0 - \gamma_0. \tag{26}$$

The deviations of the vessel position in the coordinate frame $\{b\}$ can be expressed as

$$\begin{cases} \tilde{x} = \cos\left(\psi_{C_1}\right)\tilde{N} + \sin\left(\psi_{C_1}\right)\tilde{E}, \\ \tilde{y} = -\sin\left(\psi_{C_1}\right)\tilde{N} + \cos\left(\psi_{C_1}\right)\tilde{E}. \end{cases} \tag{27}$$

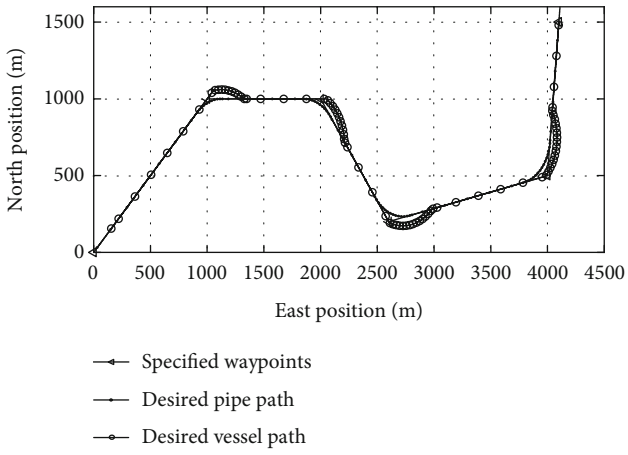

Figure 12: The specified waypoints, desired pipe path, and desired vessel path.

The deviations of the body velocity components by the vessel position deviation in the coordinate frame $\{b\}$ can be expressed as

$$\begin{cases} \tilde{u} = u_{\mathrm{d}} - u + k_{\mathrm{p}x}\tilde{x}, \\ \tilde{v} = v_{\mathrm{d}} - v + k_{\mathrm{p}y}\tilde{y}, \\ \tilde{r} = r_{\mathrm{d}} - r + k_{\mathrm{p}\psi}\tilde{\psi} + k_{\mathrm{d}\psi}\dot{\tilde{\psi}}, \end{cases} \tag{28}$$

where k_{px} is the control parameter used to convert the position deviation to the velocity deviation in surge direction. k_{py} is the control parameter used to convert the position deviation to the velocity deviation in sway direction. $k_{p\psi}$ and $k_{d\psi}$ are the control parameters used to convert the heading deviation to the rotational speed deviation.

Hence, the desired control forces generated by the propulsion system can be obtained using

$$\begin{cases} X_T = k_{\mathrm{p}u}\tilde{u} + k_{\mathrm{i}u}\int_0^t \tilde{u} + k_{\mathrm{d}u}\dot{\tilde{u}}, \\ Y_T = k_{\mathrm{p}v}\tilde{v} + k_{\mathrm{i}v}\int_0^t \tilde{v} + k_{\mathrm{d}v}\dot{\tilde{v}}, \\ N_T = k_{\mathrm{p}r}\tilde{r} + k_{\mathrm{i}r}\int_0^t \tilde{r} + k_{\mathrm{d}r}\dot{\tilde{r}}, \end{cases} \tag{29}$$

where k_{pu},k_{iu}, and k_{du} are the speed controller parameters of the dynamic positioning system in surge direction. k_{pv}, k_{iv}, and k_{dv} are the speed controller parameters of the dynamic positioning system in sway direction. k_{pr}, k_{ir}, and k_{dr} are the speed controller parameters of the dynamic positioning system in yaw direction.

4. Simulation Analysis of the Pipelaying Operation

The method presented in this study is a systematic control method, including pipeline path coding, pipeline path analysis based on the sliding matrix, mapping conversion between the desired pipeline path and the desired vessel path, the LOS guidance law of circular arc paths, and pipelaying controller design. To verify the effectiveness of the proposed method, a simulation is performed by setting a series of waypoints, pipelaying speed, crab angle, and turning radius.

A DP simulator for pipelaying operation is built using Qt software. As shown in Figure 8, the simulator consists of the waypoint table, path planning module, path guidance module, thrust allocation module, propeller system module, hydrodynamic module, environment force module, state observer module, and motion controller. It is assumed that the pipelaying water depth is a constant, and the tension of pipe tensioner is also a constant. For this simulation, the pipeline is assumed to be rigid without deformation in the pipelaying operation. Hence, the touchdown distance is also a constant.

The relevant parameters of the waypoint table need to be specified before starting pipelaying operation. All coordinates of six waypoints are set as shown in Table 3. All crab angles of the desired pipe path are set to 0 degree which means that the desired vessel heading angle is specified to be the same as the tangential angle of the desired pipeline path. The desired pipelaying speed on straight-line paths is set to 2 m/s, and the turning radius of the pipeline is set to 300 m. In addition, the touchdown distance is set to 200 m, and the desired speed on circular arc paths is set to 0.3 m/s.

Simulation environment parameters of the pipelaying operation are set as follows: the wind speed is 2 m/s, the current velocity is 1 m/s, and the wave height is 1.5 m. All environmental disturbances are assumed collinear with a direction of 40°.

4.1. Pipelaying Precision Analysis. The time step is set to 0.5 s. The results from the pipelaying simulation are shown in Figures 12–16.

For the results plotted in Figure 12, the desired pipelaying path is derived from the specified waypoints in Table 3 via the proposed method of path planning. Then, the desired vessel path is generated from the desired pipelaying path based on the parameters such as touchdown distance and turning radius in Table 3 using the presented method of pipeline path mapping. It can be seen that the vessel takes a turn at the outside of the pipeline circular arc path due to the touchdown distance and this is consistent with the theoretical results of the pipelaying path. From the simulation results shown in Figure 12, it is found that the pipelaying method of path analysis and path mapping works as expected.

The results of the vessel path obtained from the simulation and its cross-track error against the desired path are plotted in Figure 13.

As shown in Figure 13(a), the vessel path from the simulation matches well with the desired vessel path on the segments of straight-line paths and circular arc paths, even when the vessel is subjected to drift forces caused by ocean waves, wind, and currents. Therefore, these confirm that the vessel can track the desired path well through the application of the proposed method that combines path analysis, path selection, path guidance, and control technology.

As shown in Figure 13(b), the cross-track error of the vessel path is less than 0.1 m on straight-line paths. However,

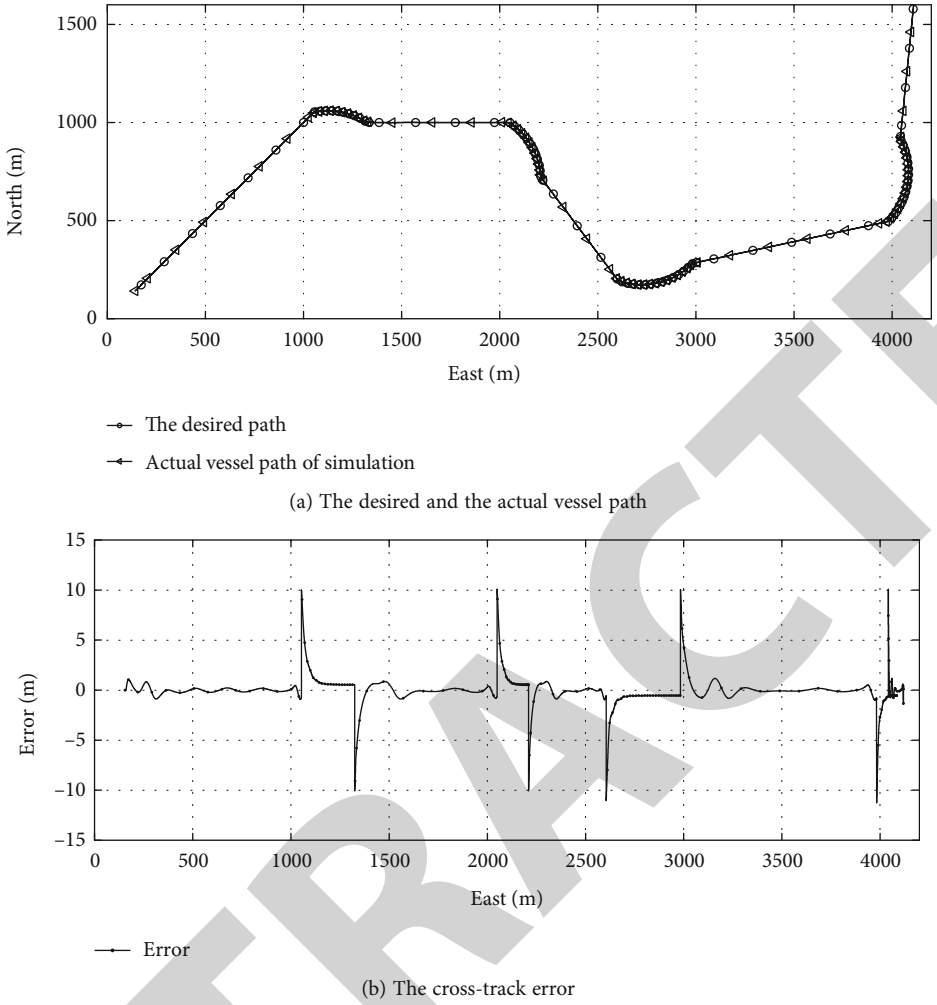

(a) The desired and the actual vessel path

(b) The cross-track error

Figure 13: Path following of the vessel.

the vessel cross-track error suddenly increases at the junction of a straight-line path and its adjacent circular arc path where the error reaches to 8.3 meters. This increased error may be the result of the continuous changing of the desired heading angle on circular arc paths, especially a sudden change of desired heading on the transition between a straight-line and its adjacent circular arc path. Then, the cross-track error gradually reduces, and finally, the path from simulation converges to the desired vessel path. Therefore, Figure 13(b) demonstrates that the proposed pipelaying controller method can make the vessel continuously track the desired vessel path.

The results of the pipe path from the simulation and its cross-track error against the desired pipe path are plotted in Figure 14.

As shown in Figure 14(a), the pipeline path from simulation matches well with the desired pipeline path during straight-line path following, and the simulated turning radius of the pipeline is the same as the specified turning radius. Therefore, it is reasonable to believe that the actual pipeline can be laid onto the desired pipelaying path by indirectly controlling the vessel motion. Additionally, Figure 14(a) also demonstrates that continuous pipelaying operation can be achieved via the proposed pipelaying control method. Consequently, the proposed method can be applied to various laying paths of pipelines and it is robust.

The cross-track error of the pipe path is shown in Figure 14(b). The cross-track error is less than 0.5 m on the segments of straight-line paths. However, the cross-track error suddenly increases at the junction of a straight-line path and its adjacent circular arc path. The maximum value of the cross-track error of the pipeline is approximately 9.5 m, which may be caused by a sudden change of the desired heading when the vessel is traveling between a straight-line path to its adjacent circular arc path. Besides, it may also be caused by the assumption that the pipe is rigid, and the cross-track error of the pipeline should be less than this value if the pipeline dynamic model [3, 6, 36] is considered. However, the cross-track error is gradually converged to zero when the vessel travels past the transition points.

4.2. Speed Analysis in Pipelaying Operation. The curves of speed performance during pipelaying operation are shown in Figure 15.

The pipelaying speed is 2 m/s on straight-line paths, and the speed is decreased to 0.3 m/s on the circular arc paths, which are consistent with the specified speed in the

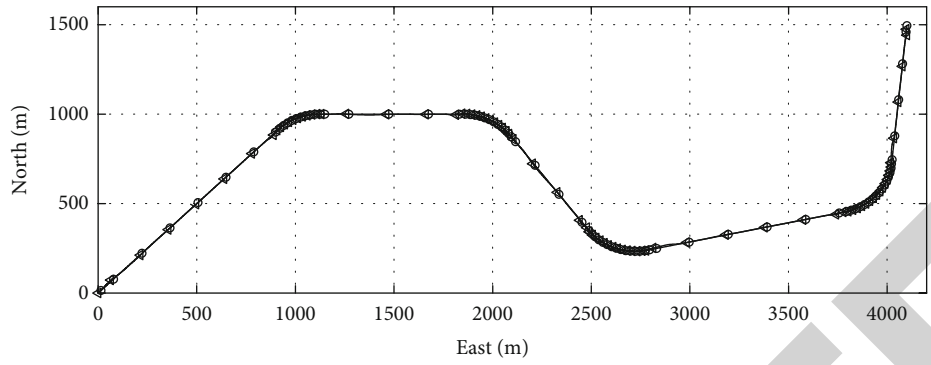

(a) The desired and the actual pipelaying path

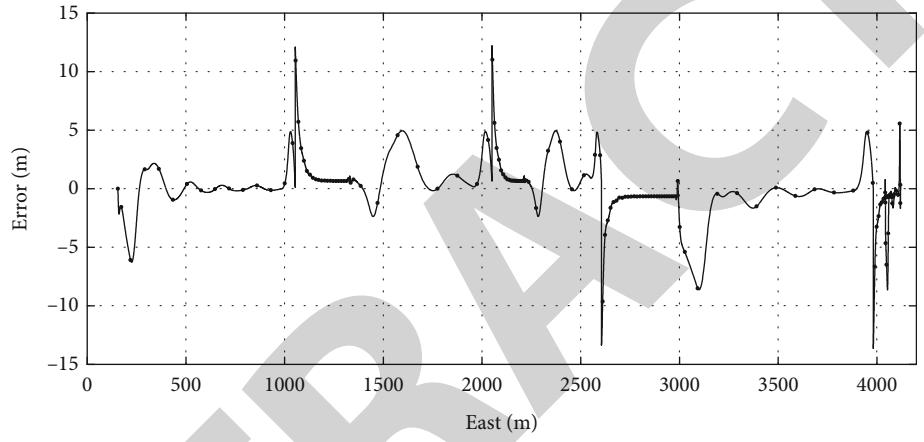

(b) The cross-track error

Figure 14: The pipelaying results of the pipeline.

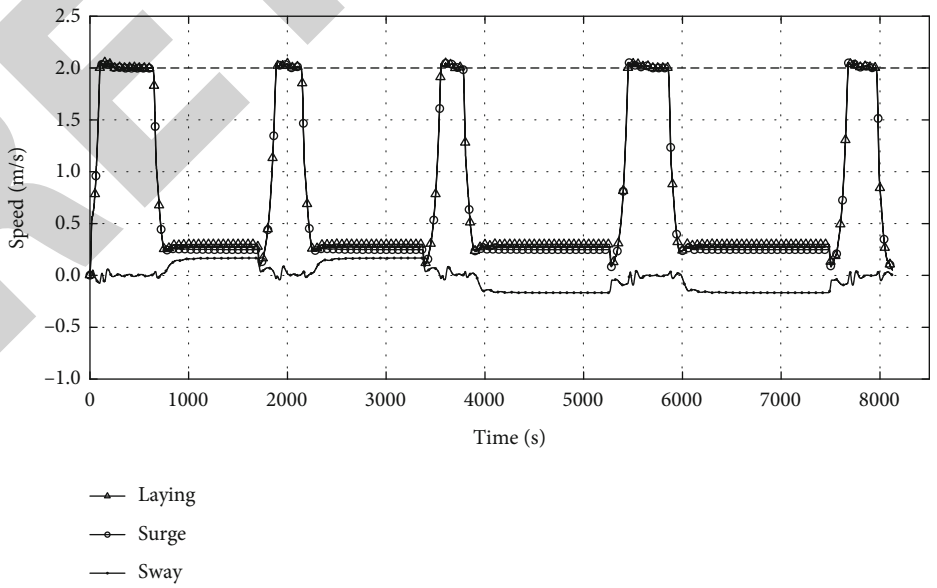

Figure 15: The vessel speed and pipelaying speed.

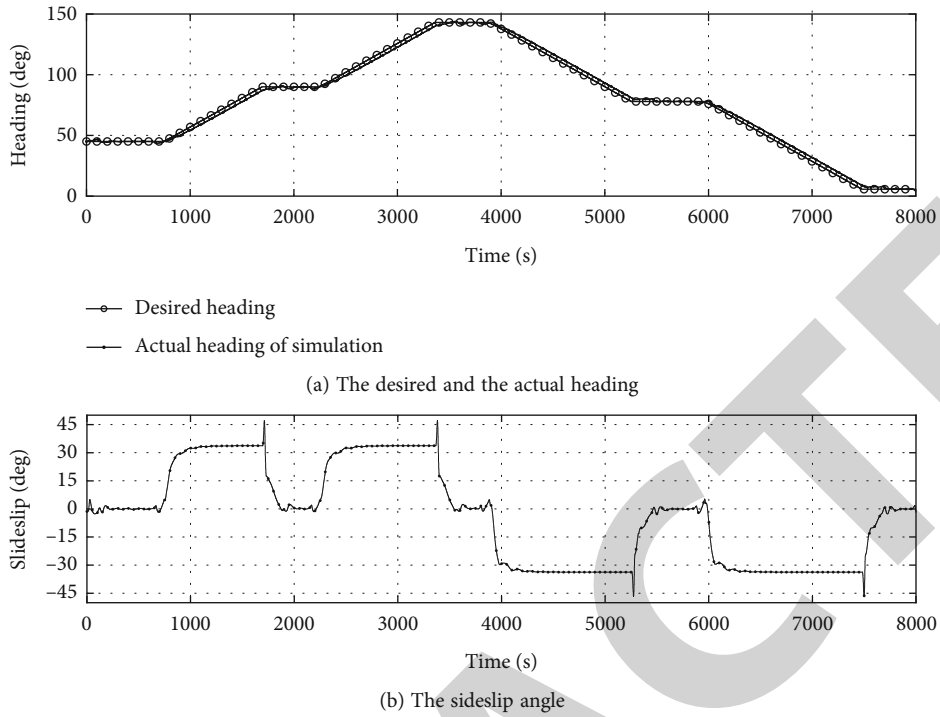

(a) The desired and the actual heading

(b) The sideslip angle

Figure 16: The vessel heading angle and sideslip angle.

waypoint table. As shown in Figure 15, the vessel speed along the surge direction is close to the pipelaying speed when the vessel is moving along a straight-line path. However, there is a relatively constant offset between the vessel speed along the surge direction and the pipelaying speed when the vessel is moving along a circular arc path, which is due to the vessel sway speed on the circular arc paths. Figure 15 also shows that the vessel speed along the sway direction is up to 0.18 m/s; this is the result of continuous changing of the desired heading angle which is consistent with the tangent of the desired pipe path despite that the predefined pipelaying speed on circular arc paths is reduced to 0.3 m/s. It is noticed that the vessel speed along the sway direction is decreased to zero on the straight-line paths. Hence, it is proved that the pipelaying controller designed in this study can control the vessel position and speed simultaneously during pipelaying operation.

4.3. Analysis of the Heading and Sideslip Angle. The vessel attitude performance in the pipelaying simulation, including the heading angle and sideslip angle, is shown in Figure 16.

As shown in Figure 16(a), the desired heading angle on the segments of the straight-line path is a constant, which is equal to the direction of the straight-line path. The desired heading angle on the segments of circular arc paths is a straight line with a constant slope, which is equal to the tangent direction of circular arc paths. Due to the limitation of the response speed of the vessel propulsion system, the propellers cannot immediately produce the desired thrusts, and there is always a time lag between the actual heading angle and the desired heading angle during path following on circular arc paths. However, the time lag is quite small. Therefore, it proves that the actual heading angle can track the desired value during operation using the designed pipelaying controller.

As shown in Figure 16(b), the sideslip angle fluctuates around zero on the segments of straight-line paths, which may be caused by the environmental forces from wind, wave, and currents. However, the vessel actual heading angle converges to the tangential direction of the desired circular arc paths and it is obtained by allowing a certain sideslip angle. The sideslip angle increases from 0° to 33° or decreases from 0 to -33°when the vessel is traveling along a circular arc path.

The proposed method, including path planning, path guidance, path tracking, and controlling, based on the sliding matrix for pipelaying operation in the study is effective. It is also proved by pipelaying simulation and analysis that the method is accurate in terms of the actual path, pipelaying speed, heading angle, and sideslip angle. The pipeline can be continuously laid onto the predefined path according to the specified pipe path, crab angle, pipelaying speed, and turning radius.

5. Conclusions

Through the operation simulation of pipelaying by DP ship and the analysis of the simulation results of pipeline trajectory, ship trajectory, pipelaying accuracy, pipelaying speed, and heading angle, the following conclusions can be obtained:

(1) A systematic method of pipelaying motion planning, guidance, and control of DP ship is proposed in this paper, which can control the pipelaying ship to switch smoothly between straight line and curve path, automatically update the path and relevant

control information along the waypoint table, and realize the continuous laying of offshore pipeline at a specified speed

(2) A pipeline path analysis and coding method based on a sliding matrix are proposed, which can realize automatic pipeline path analysis, automatic coding storage, and path mapping. With the progress of pipelaying, the relevant path and control information are automatically updated, which simplifies the preprocessing of the whole waypoint table and improves the automatic analysis ability of DP pipelaying path

(3) A circular path guidance method is proposed, and a multiobjective motion controller of DP ship is designed, which can effectively control the position, turning radius, speed, and attitude of DP pipelaying ship

Relevant simulation results show that the control method of pipelaying is effective and works reasonably well. This method is adopted in this paper to achieve the continuous pipelaying of the DP vessel, and it can also provide a valuable reference for path planning, guidance, and path tracking control of other surface vessels and underwater vehicles.

Data Availability

The raw data supporting the conclusions of this article will be made available by the authors, without undue reservation.

Conflicts of Interest

The authors declared that they have no conflicts of interest regarding this work.

Acknowledgments

This work was supported by the National Key Research and Development Program of China (2018YFC1406000).

References

[1] T. I. Fossen, *Handbook of Marine Craft Hydrodynamics and Motion Control*, Wiley, New York, USA, 2011.

[2] E. P. Heerema, "Recent achievements and present trends in deep-water pipe-lay systems," in *Proceedings of the 37th Offshore Technology Conference, OTC*, p. 17627, 2005.

[3] S. Ai, L. Sun, and L. Tao, "Modeling and simulation of deepwater pipeline S-lay with coupled dynamic positioning," *Journal of Offshore Mechanics and Arctic Engineering*, vol. 140, no. 5, pp. 1–10, 2018.

[4] P. Xu, Z. Du, F. Huang, and A. Javanmardi, "Numerical simulation of deepwater S-lay and J-lay pipeline using vector form intrinsic finite element method," *Ocean Engineering*, vol. 234, p. 09039, 2021.

[5] M. Panda, B. Das, B. Subudhi, and B. B. Pati, "A comprehensive review of path planning algorithms for autonomous underwater vehicles," *International Journal of Automation and Computing*, vol. 17, no. 3, pp. 321–352, 2020.

[6] Y. Ma, Y. Gong, C. Xiao, Y. Gao, and J. Zhang, "Path planning for autonomous underwater vehicles: an ant colony algorithm incorporating alarm pheromone," *IEEE Transactions on Vehicular Technology*, vol. 68, no. 1, pp. 141–154, 2019.

[7] N. A. Shneydor and D. Ingenieu, *Missile Guidance and Pursuit: Kinematics, Dynamics and Control*, Horwood Publishing Limited, Chichester, 1998.

[8] M. Breivik, "Topics in guided motion control of marine vehicles," in *Recent achievements and present trends in deepwater pipe-lay systems*, pp. 29–56, Doctor Dissertation of Norway University of Science and Technology, 2010.

[9] L. E. Dubin, "On curves of minimal length with a constraint on average curvature, and with prescribed initial and terminal positions and tangents," *Amer. J. Math.*, vol. 79, no. 3, pp. 497–516, 1957.

[10] R. T. Farouki and T. Sakkalis, "Pythagorean hodographs," *IBM Journal of Research and Development*, vol. 34, no. 5, pp. 736–752, 1990.

[11] H. Bruyninckx and D. Reynaerts, "Path planning for mobile and hyper-redundant robots using Pythagorean hodograph curves," in *1997 8th International Conference on Advanced Robotics. Proceedings. ICAR'97*, pp. 595–600, Monterey, CA, USA, 1997.

[12] A. M. Lekkas and T. I. Fossen, "Integral LOS path following for curved paths based on a monotone cubic Hermite spline parametrization," *IEEE Transactions on Control Systems Technology*, vol. 22, no. 6, pp. 2287–2301, 2014.

[13] M. Fu, A. Zhang, and J. Xu, "Adaptive dynamic surface tracking control for dynamic positioning cable laying vessel," in *2012 IEEE International Conference on Automation and Logistics*, pp. 266–271, Zhengzhou, China, 2012.

[14] M. Fu, B. Wu, and X. Zhang, "Modeling and analysis of trajectory tracking for DP vessel pipelaying based on back-stepping sliding mode method," *The Journal of New Industrialization*, vol. 4, no. 3, pp. 17–22, 2014.

[15] R. Rout, R. Cui, and Z. Han, "Modified line-of-sight guidance law with adaptive neural network control of underactuated marine vehicles with state and input constraints," *IEEE Transactions on Control Systems Technology*, vol. 28, no. 5, pp. 1902–1914, 2020.

[16] A. M. Lekkas and T. I. Fossen, *Line-of-sight guidance for path-following of marine vehicles*, Lamber Academic Publishing, 2013.

[17] A. M. Lekkas and T. I. Fossen, "A time-varying lookahead distance guidance law for path following," *IFAC Proceedings Volumes*, vol. 45, no. 27, pp. 398–403, 2012.

[18] T. I. Fossen, K. Y. Pettersen, and R. Galeazzi, "Line-of-sight path following for Dubins paths with adaptive sideslip compensation of drift forces," *IEEE Transactions on Control Systems Technology*, vol. 23, no. 2, pp. 820–827, 2015.

[19] E. Peymani and T. I. Fossen, "Direct inclusion of geometric errors for path maneuvering of marine craft," *IFAC Proceedings Volumes*, vol. 45, no. 27, pp. 293–298, 2012.

[20] E. Peymani and T. I. Fossen, "2D path following for marine craft: a least-square approach," *IFAC Proceedings Volumes*, vol. 46, no. 23, pp. 98–103, 2013.

[21] S. Moe, K. Y. Pettersen, T. I. Fossen, and J. T. Gravdahl, "Line-of-sight circular arc path following for underactuated USVs and AUVs in the horizontal plane under the influence of ocean

currents," in *24th Mediterranean Conference on Control and Automation*, pp. 38–45, 2016.

[22] S. Heshmati-Alamdari, A. Nikou, and D. V. Dimarogonas, "Robust trajectory tracking control for underactuated autonomous underwater vehicles in uncertain environments," *IEEE Transactions on Automation Science and Engineering*, vol. 18, no. 3, pp. 1288–1301, 2021.

[23] J. Nie and X. Lin, "Improved adaptive integral line-of-sight guidance law and adaptive fuzzy path following control for underactuated MSV," *ISA Transactions*, vol. 94, pp. 151–163, 2019.

[24] B. Abdurahman, A. Savvaris, and A. Tsourdos, "Switching LOS guidance with speed allocation and vertical course control for path-following of unmanned underwater vehicles under ocean current disturbances," *Ocean Engineering*, vol. 182, pp. 412–426, 2019.

[25] H. C. Lamraoui and Z. Qidan, "Path following control of fully-actuated autonomous underwater vehicle in presence of fast-varying disturbances," *Applied Ocean Research*, vol. 86, pp. 40–46, 2019.

[26] J. du, X. Hu, M. Krstić, and Y. Sun, "Robust dynamic positioning of ships with disturbances under input saturation," *Automatica*, vol. 73, pp. 207–214, 2016.

[27] C. Yu, X. Xiang, L. Lapierre, and Q. Zhang, "Nonlinear guidance and fuzzy control for three-dimensional path following of an underactuated autonomous underwater vehicle," *Ocean Engineering*, vol. 146, pp. 457–467, 2017.

[28] H. Xinjing, L. Yibo, D. Fei, and J. Shijiu, "Horizontal path following for underactuated AUV based on dynamic circle guidance," *Robotica*, vol. 35, no. 4, pp. 876–891, 2017.

[29] A. Loginov, A. Proskurnikov, E. Ambrosovskaya, and D. Romaev, "DP systems for track control of dredging vessels," *IFAC Proceedings Volumes*, vol. 45, no. 27, pp. 453–458, 2012.

[30] X. Shi, W. Xie, M. Fu, and X. Sun, "Terminal sliding mode tracking control for dynamic positioning J-laying vessel," in *Proceeding of IEEE International Conference on Automation and Logistics*, pp. 293–298, 2011.

[31] A. J. Healey and D. Lienard, "Multivariable sliding mode control for autonomous diving and steering of unmanned underwater vehicles," *IEEE Journal of Oceanic Engineering*, vol. 18, no. 3, pp. 327–339, 1993.

[32] D. Mu, G. Wang, Y. Fan, Y. Bai, and Y. Zhao, "Fuzzy-based optimal adaptive line-of-sight path following for underactuated unmanned surface vehicle with uncertainties and time-varying disturbances," *Mathematical Problems in Engineering*, vol. 2018, Article ID 7512606, 12 pages, 2018.

[33] R. Rout and B. Subudhi, "Design of line-of-sight guidance law and a constrained optimal controller for an autonomous underwater vehicle," *IEEE Transactions on Circuits and Systems II: Express Briefs*, vol. 68, no. 1, pp. 416–420, 2021.

[34] G. A. Jensen, *Modeling and Control of Offshore Pipelay Operations, [Ph.D. thesis]*, Norwegian University of Science and Technology, 2009.

[35] G. A. Jensen, N. Saftrom, T. D. Nguyen, and T. I. Fossen, "Modeling and control of offshore pipelay operations based on a finite strain pipe model," in *2009 American Control Conference*, pp. 4711–4722, St. Louis, MO, USA, 2009.

[36] M. Szczotka, "Pipe laying simulation with an active reel drive," *Ocean Engineering*, vol. 37, no. 7, pp. 539–548, 2010.